

Magnetic Propulsion Force Calculation of a 2-DoF Large Stroke Actuator for High-Precision Magnetic Levitation System

Mousa Lahdo^{1,2}, Tom Ströhla², and Sergej Kovalev¹

¹Department of Informatics, Electrical Engineering and Mechatronics
University of Applied Sciences Mittelhessen, Friedberg, 61169, Germany
mousa.lahdo@iem.thm.de, sergej.kovalev@iem.thm.de

²Department of Mechatronics
Ilmenau University of Technology, Ilmenau, 98693, Germany
tom.stroehla@tu-ilmenau.de

Abstract — The design of high-precision magnetic levitation positioning systems requires fast electromagnetic models. Since three-dimensional finite element method (3D-FEM) is very time-consuming, in order to calculate magnetic forces, an interesting alternative is to determine the forces semi-analytically due to the high accuracy with a short calculation time. In this paper, a new compact semi-analytical equation for determining the magnetic propulsion forces of a new ironless two degrees of freedom (2-DoF) actuator for a high-precision magnetic levitation system is presented. The derived equation is based on the magnetic scalar potential and the Lorentz force law. An important result is that this new expression takes also the position dependence of the propulsion forces over the whole planar stroke into account. The calculated propulsion forces from the derived equations and the verification by 3D-FEM (Maxwell 3D) are presented in this paper as well.

Index Terms — Analytical calculation, ironless actuator, Lorentz force, magnetic levitation, magnetic scalar potential, Maxwell 3D.

I. INTRODUCTION

Due to the ongoing miniaturization of electronic components, many modern applications, such as the semiconductor manufacturing or nanotechnology, requires vacuum compatible planar positioning systems with long planar strokes and precisions up to the nanometer (nm) range [1]. One promising solution to achieve these requirements is the combination of multiple electrodynamic linear actuators with active magnetic guidances in a triangular or rectangular configuration [2].

These high-precision 6-DoF magnetic levitation positioning systems can position objects precisely up to the nm range without any contact in multiple degrees of

freedom with only one moving element [3]. In order to eliminate hysteresis effects, flux saturation and eddy-currents, obtained from ferromagnetic materials, currently most of the high-precision magnetic levitation positioning systems known in the literature are realized with ironless actuators [3]. These ironless actuators consist usually of a stator with air-core coils and a mover with either a Halbach array [4] or a single permanent magnet [5]. The main advantage of the iron-free structure of these systems are the linear relationship between the currents and forces and the fast current changes in the air-core coils, which allows the realization of simple and highly dynamic control algorithms.

For the purpose of designing, analyzing and optimizing of such systems, often 3D-FEM are required and used because the geometry of such positioning systems is a complex 3D problem [6-7]. However, the main problem of 3D-FEM is that it requires partly several hours to obtain a solution, since it needs extremely fine meshing within the air gap as well as the surrounding medium in order to obtain accurate results of the forces and magnetic fields. Consequently, alternative solutions are required in order to calculate magnetic forces and fields very fast [8].

One interesting alternative is the calculation of the magnetic forces and fields analytically, because it combines high accuracy with a very low computational time compared to 3D-FEM [9-11]. Therefore, many scientists calculate forces in planar positioning systems and in ironless systems analytically instead using 3D-FEM [12-14]. Mostly, they focus on the calculation of the repulsive levitation forces of magnetic guidances. However, because of the inherently unstable behavior of repulsive magnetic guidances, the moving magnet experiences, in addition to the levitation force, also a destabilizing force, that intends to push the permanent magnet laterally away from the center position. Thus, the determination of these undesired propulsion forces

are a crucial task, since they must compensate from propulsion actuators in order to restore the lateral stability and to move and position the mover simultaneously.

In this paper, attention is given to the semi-analytical calculation of the planar propulsion forces of a novel 2-DoF actuator presented in [3]. The main contributions are new expressions, which consider the position dependence of the desired propulsion force and the planar destabilizing propulsion forces over the whole planar stroke.

II. 2-DOF ACTUATOR

The actuator under investigation is shown in Fig. 1. This novel 2-DoF actuator for 6-DoF high-precision magnetic levitation systems is proposed in order to overcome the limitations of Halbach arrays and reluctance actuators [3]. It consists of air-core propulsion and guiding coils generating two perpendicular forces (levitation and propulsion) on a single moving magnet. This actuator configuration reduces the mover mass significantly and consequently the power consumption of the guiding coil. A 6-axis motion can be realized with only three or four of such actuators in a triangular or rectangular configuration [3]. As mentioned, the magnetic guiding coil generates not only a desired repulsive levitation force, but also an undesired destabilizing propulsion force. Figure 2 shows a more detailed illustration of this unstable behavior.

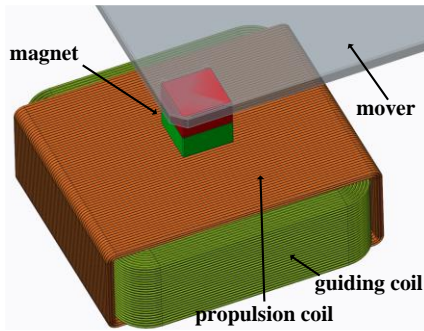


Fig. 1. Ironless 2-DoF actuator.

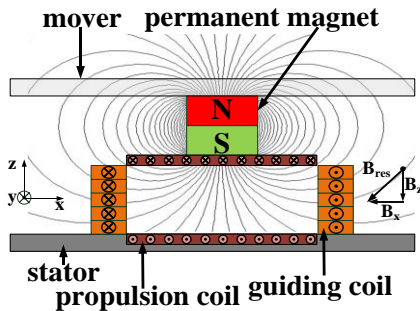


Fig. 2. Generation of the propulsion and levitation force.

As can be seen, the magnetic field generated by the permanent magnet creates flux density components in the x - and z -direction. The x -component of the magnetic flux density creates the desired levitation force, i.e., the motion of the mover along the z -direction is stable. This is because as the air gap increases, the repulsive levitation force decreases and thus, the gravitational force restores the mover in the equilibrium position. Nevertheless, the z -component of the magnetic flux density is responsible for a destabilizing propulsion force that intends to push the permanent magnet away from the equilibrium position. This instability is consistent with Earnshaw's theorem, which states that a stable levitation based only on static magnetic forces between dc coils and permanent magnets is never stable in all directions simultaneously [15]. Consequently, a stable levitation can only be achieved by an additional propulsion actuator in combination with a control system.

However, the total force acting on the permanent magnet is generated according to the electrodynamic principle (Lorentz force) and can be calculated using the Lorentz force formula:

$$\mathbf{F} = \int_{V_{coil}} \mathbf{J} \times \mathbf{B} dV_{coil}, \quad (1)$$

where \mathbf{J} is the current density in the coil, \mathbf{B} the magnetic flux density generated by the neodym-iron-boron ($NdFeB$) permanent magnet and dV_{coil} represents the small volume element in the coils.

A. Analytical calculation of the magnetic flux density

In order to evaluate the Lorentz force according to (1), the first important step is the calculation of the magnetic flux density of the $NdFeB$ permanent magnet inside the coil volume. One possible calculation approach known in the literature is based on the magnetic scalar potential, which results in a reduction of the magnet to a distribution of fictive magnetic charges (magnetic surface charge model) (Fig. 3) [13]. The magnetic surface charge model is derived from the magnetic scalar potential φ . The starting point is Ampere's law for current-free region:

$$\nabla \times \mathbf{H} = 0, \quad (2)$$

where ∇ is the Nabla-Operator and \mathbf{H} is the magnetic field strength.

Since (2) is rotation-free, from a mathematical point of view, the magnetic field strength can be described by introducing a magnetic scalar potential φ [16]:

$$\mathbf{H} = -\nabla \cdot \varphi. \quad (3)$$

Inserting the constitutive relation,

$$\mathbf{B} = \mu_0 \cdot (\mathbf{H} + \mathbf{M}), \quad (4)$$

where μ_0 is the vacuum permeability and \mathbf{M} the magnetization of the permanent magnet into Gauss's law for magnetism:

$$\nabla \cdot \mathbf{B} = 0, \quad (5)$$

yields,

$$\nabla \cdot \mathbf{H} = -\nabla \cdot \mathbf{M}. \quad (6)$$

By introducing a fictive magnetic charge density $\rho = -\nabla \cdot \mathbf{M}$ and using the magnetic scalar potential φ , this results in:

$$\nabla^2 \cdot \varphi_m = -\rho. \quad (7)$$

Under the condition that there are no boundary surfaces in the whole volume, that is $\mu = \text{const.}$, and under the assumption of ideal magnets, which are characterized by a fixed and uniform magnetization in the volume of the magnets, the solution for the magnetic scalar potential φ is as follows [13]:

$$\varphi = \frac{1}{4\pi} \oint_{S_{mag}} \frac{\mathbf{M}(\mathbf{r}_Q) \cdot \mathbf{n}}{|\mathbf{r} - \mathbf{r}_Q|} dS_{mag}, \quad (8)$$

where dS_{mag} is the surface that bounds the volume V of the magnet, $\mathbf{r} = \{x, y, z\}$ describes the point of evaluation and $\mathbf{r}_Q = \{x_Q, y_Q, z_Q\}$ describes the position of the source. In free-space, the magnetic flux density can be expressed as:

$$\mathbf{B} = \mu_0 \mathbf{H}, \quad (9)$$

and finally with (8) substitute into (3), (9) becomes:

$$\mathbf{B} = \frac{\mu_0}{4\pi} \oint_{S_{mag}} \mathbf{M}(\mathbf{r}_Q) \cdot \mathbf{n} \cdot \frac{(\mathbf{r} - \mathbf{r}_Q)}{|\mathbf{r} - \mathbf{r}_Q|^3} dS_{mag}. \quad (10)$$

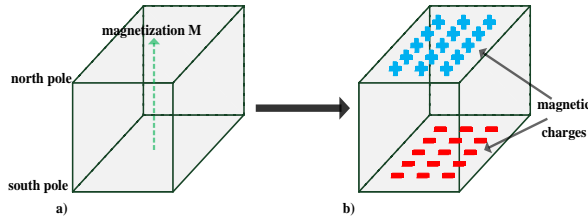


Fig. 3. *NdFeB* permanent magnet (a) and magnetic surface charge model (b).

B. Destabilizing force calculation of the guiding coil

Using (10) and inserting into (1), the total Lorentz force can be generally written as:

$$\mathbf{F} = \int_{V_{coil}} \mathbf{J} \times \left(\frac{\mu_0}{4\pi} \oint_{S_{mag}} \mathbf{M}(\mathbf{r}_Q) \cdot \mathbf{n} \cdot \frac{(\mathbf{r} - \mathbf{r}_Q)}{|\mathbf{r} - \mathbf{r}_Q|^3} dS_{mag} \right) dV_{coil}. \quad (11)$$

In order to calculate the destabilizing propulsion force, we split the whole guiding coil in four identical coil sections according to Fig. 4, where two of the coil sections generate a force in the x -direction (CS1 and CS3), and the remaining coil sections (CS2 and CS4) in the y -direction, respectively. For calculation of the propulsion force in x -direction generated by CS1 and CS3, we determine the z -component of the magnetic flux density B_z :

$$B_z = \mathbf{B} \cdot \mathbf{e}_z = \frac{\mu_0}{4\pi} \oint_{S_{mag}} \mathbf{M}(\mathbf{r}_Q) \cdot \mathbf{n} \cdot \frac{(\mathbf{r} - \mathbf{r}_Q)}{|\mathbf{r} - \mathbf{r}_Q|^3} \cdot \mathbf{e}_z dS_{mag}, \quad (12)$$

and assume also a constant and uniform volume current density in the y -direction (see Fig. 4 (b)):

$$\mathbf{J} = \frac{N \cdot I}{b_{ai} \cdot h} \cdot \mathbf{e}_y, \quad (13)$$

where N is the number of coil turns, I the current through the coil, $b_{ai} \cdot h$ the cross sectional area and \mathbf{e}_y is the unit vector in the y -direction. Under consideration of the parameters, shown also in Fig. 4, the destabilizing propulsion force in x -direction as a function of the current mover position over the whole planar stroke can be calculated according to (14), shown at the bottom of the next page.

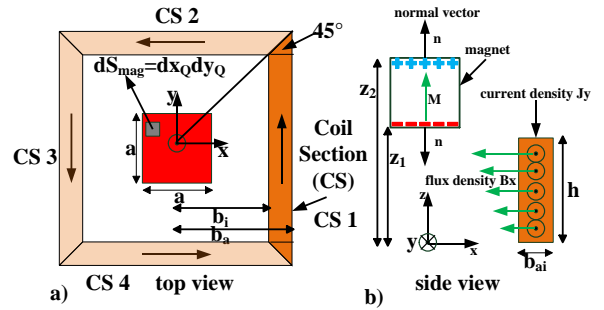


Fig. 4. Geometry of the magnetic guiding coil.

This derived equation is semi-analytical, because this equation requires besides an analytical integration, also a numerical integration.

In the exact manner, we derive (15) in order to calculate the destabilizing propulsion force along the y -direction. Since the undesired destabilizing propulsion forces along the x - and y -direction acts simultaneously on the permanent magnet, the superposition of both forces must be applied in order to determine the total destabilizing force:

$$F_{xy} = \sqrt{F_x^2 + F_y^2}. \quad (16)$$

C. Force calculation of the propulsion coil

The propulsion coil in the 2-DOF actuator contributes towards the desired motion in the planar stroke. The magnitude of the propulsion force component must be bigger than the magnitude of the destabilizing propulsion force components generated by the guiding coil, in order to counteract these destabilizing forces and to move and position the mover precisely within the planar stroke. Similar to the guiding coil, we divide the propulsion coil into four sections as shown in Fig. 5. Only CS2 generates the propulsion force in the desired

direction, whereas the other coil sections generate a force in the opposite direction. To determine the desired propulsion force acting in the x -direction as a function of the current mover position, we calculate the force components of the coil sections using (17–19) with the parameters also shown in Fig. 5. The actual propulsion force on the magnet can be calculated using (20):

$$F_{x,prop} = F_{CS_2} - F_{CS_4} - F_{CS_{13}}. \quad (20)$$

$$F_x = \frac{\mu_0 M N \cdot I}{4\pi b_{ai} h} \left(\sum_{\alpha=0}^1 \sum_{\beta=1}^2 \int_{-\frac{a}{2}+yp}^{\frac{a}{2}+yp} \int_{-\frac{a}{2}+xp}^{\frac{a}{2}+xp} \int_{-\frac{h}{2}}^{\frac{h}{2}} \int_{(1-\alpha) \cdot b_i - \alpha \cdot b_a}^{(1-\alpha) \cdot b_a - \alpha \cdot b_i} \int_{-x}^x \frac{-(-1)^\beta (z - z_\beta)}{\left(\sqrt{(x - x_Q)^2 + (y - y_Q)^2 + (z - z_\beta)^2}\right)^3} dy dx dz dx_Q dy_Q, \quad (14)$$

$$F_y = \frac{\mu_0 M N \cdot I}{4\pi b_{ai} h} \left(\sum_{\alpha=0}^1 \sum_{\beta=1}^2 \int_{-\frac{a}{2}+yp}^{\frac{a}{2}+yp} \int_{-\frac{a}{2}+xp}^{\frac{a}{2}+xp} \int_{-\frac{h}{2}}^{\frac{h}{2}} \int_{(1-\alpha) \cdot b_i - \alpha \cdot b_a}^{(1-\alpha) \cdot b_a - \alpha \cdot b_i} \int_{-y}^y \frac{-(-1)^\beta (z - z_\beta)}{\left(\sqrt{(x - x_Q)^2 + (y - y_Q)^2 + (z - z_\beta)^2}\right)^3} dx dy dz dx_Q dy_Q, \quad (15)$$

$$F_{CS_2} = \frac{\mu_0 M N_p \cdot I_p}{4\pi b_c h_{c1}} \left(\int_{-\frac{a}{2}+yp}^{\frac{a}{2}+yp} \int_{-\frac{a}{2}+xp}^{\frac{a}{2}+xp} \int_{\frac{h_c}{2}}^{\frac{h_c}{2}+h_{c1}} \int_{-\frac{b_c}{2}}^{\frac{b_c}{2}} \int_{-\frac{b_d}{2}}^{\frac{b_d}{2}} \sum_{\beta=1}^2 \frac{-(-1)^\beta (z - z_{\beta p})}{\left(\sqrt{(x - x_Q)^2 + (y - y_Q)^2 + (z - z_{\beta p})^2}\right)^3} dy dx dz dx_Q dy_Q, \quad (17)$$

$$F_{CS_4} = \frac{\mu_0 M N_p \cdot I_p}{4\pi b_c h_{c1}} \left(\int_{-\frac{a}{2}+yp}^{\frac{a}{2}+yp} \int_{-\frac{a}{2}+xp}^{\frac{a}{2}+xp} \int_{-\frac{h_c}{2}}^{\frac{h_c}{2}} \int_{-\frac{b_c}{2}}^{\frac{b_c}{2}} \int_{-\frac{b_d}{2}}^{\frac{b_d}{2}} \sum_{\beta=1}^2 \frac{-(-1)^\beta (z - z_{\beta p})}{\left(\sqrt{(x - x_Q)^2 + (y - y_Q)^2 + (z - z_{\beta p})^2}\right)^3} dy dx dz dx_Q dy_Q, \quad (18)$$

$$F_{CS_{13}} = \frac{\mu_0 M N_p \cdot I_p}{4\pi b_c h_{c1}} \left(\sum_{\alpha=0}^1 \sum_{\beta=1}^2 \int_{-\frac{a}{2}+yp}^{\frac{a}{2}+yp} \int_{-\frac{a}{2}+xp}^{\frac{a}{2}+xp} \int_{-\frac{h_c}{2}}^{\frac{h_c}{2}} \int_{(1-\alpha) \cdot (\frac{b_d}{2} - k) - \alpha \cdot \frac{b_d}{2}}^{(1-\alpha) \cdot \frac{b_d}{2} - \alpha \cdot (\frac{b_d}{2} - k)} \int_{-\frac{b_c}{2}}^{\frac{b_c}{2}} \frac{-(-1)^\beta (y - y_Q)}{\left(\sqrt{(x - x_Q)^2 + (y - y_Q)^2 + (z - z_{\beta p})^2}\right)^3} \right. \quad (19)$$

$\cdot dx dy dz dx_Q dy_Q.$

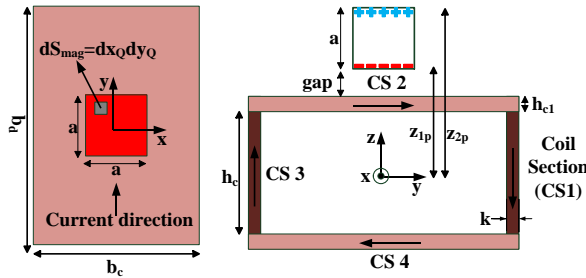


Fig. 5. Geometry of the magnetic propulsion coil.

III. RESULTS AND DISCUSSION

As already mentioned, the quintuple equations are semi-analytical, i.e., after two consecutive analytical integrations with the Symbolic Math Toolbox of MATLAB, it is difficult to express the remaining

The results based on our proposed equations can be used to design the control system. One possible approach is to store the Lorentz force values acting on the permanent magnet as a function of the current mover position in a look up table. Another approach is to use a polynomial function to fit the forces versus x and y . Anyway, both approaches can greatly help in the design of the control system.

expression in an analytical form. Thus, after the analytical integration, we convert the remaining expression in a function handle using *matlabFunction* and used the intern numerical integration function *integral3* to evaluate the remaining triple integral. The function of the numerical integration is used with the default settings. In order to simplify the calculation procedure, a MATLAB program is written which contains the analytical and numerical integration. Based on our MATLAB program, the destabilizing propulsion forces are calculated in millimeters in the horizontal plane from -20 mm to $+20$ mm (Fig. 6).

In order to validate the semi-analytical equations, the Lorentz forces acting on the coils were also predicted using 3D-FEM (Fig. 7). The parameters and dimensions required for the numerical and semi-analytical calculation are given in Table 1.

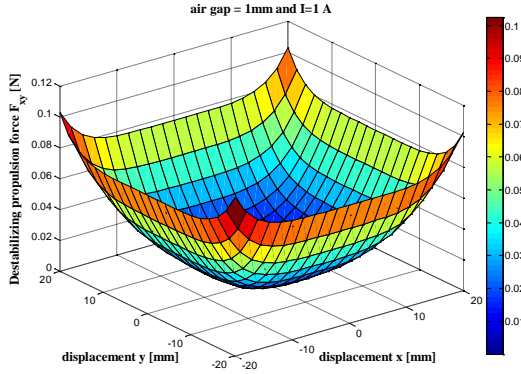


Fig. 6. Calculated destabilizing force.

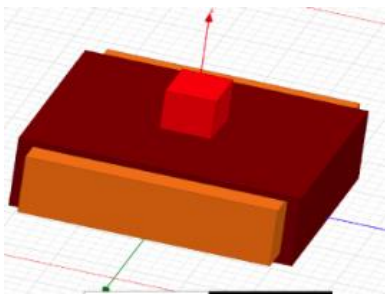


Fig. 7. 3D-FEM model (Maxwell 3D).

Table 1: Parameters for the force calculation

Parameter	Symbol	Value	Unit
Number of turns	N/N_p	250 / 200	
Current	I/I_p	1 / 1	A
Remanence of PM	$\mu_0 M$	1.44	Vs/m ²
Coil thickness	b_{ai}/b_c	10 / 80	mm
Coil height	$h/h_c/k/h_c$	30 / 30 / 5 / 3	mm
Coil length	b_d	110	mm
Magnet length	a	20	mm
Coil inner side	b_i	40	mm
Coil outer side	b_a	50	mm
Neg. magnetic charges height	z_1/z_{1p}	34 / 19	mm
Pos. magnetic charges height	z_2/z_{2p}	54 / 39	mm

The comparison of the destabilizing force-displacement curves using the derived equations and 3D-FEM is shown in Fig. 8, and the comparison of the propulsion force generated by the propulsion coil can be seen in Fig. 9, respectively. It can be observed in both figures, that the numerical and semi-analytical computation shows a very good agreement. The max. error between the solutions of our equation and the numerical ones in all investigated curves is below 1%. In order to determine the forces over the whole planar stroke, the calculation time of the 3D-FEM takes several hours, whereas the semi-analytical approach with MATLAB

takes only a few seconds. Consequently, our proposed method is a very fast alternative to the time-consuming 3D-FEM and can be used for designing and optimizing the 2-DoF actuator. Moreover, the presented theory in this paper can be easily adopted for other ironless PM-actuators.

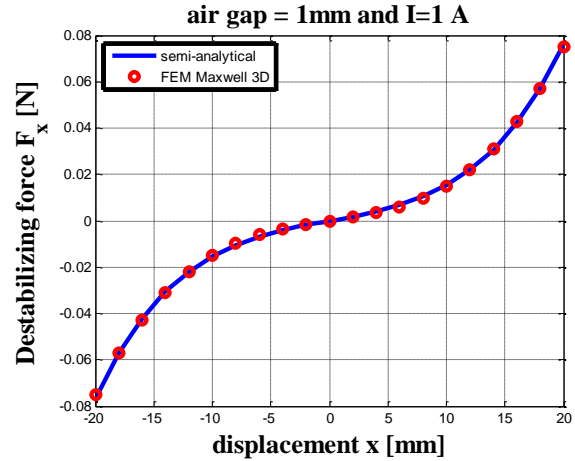


Fig. 8. Force-displacement curve of the guiding coil.

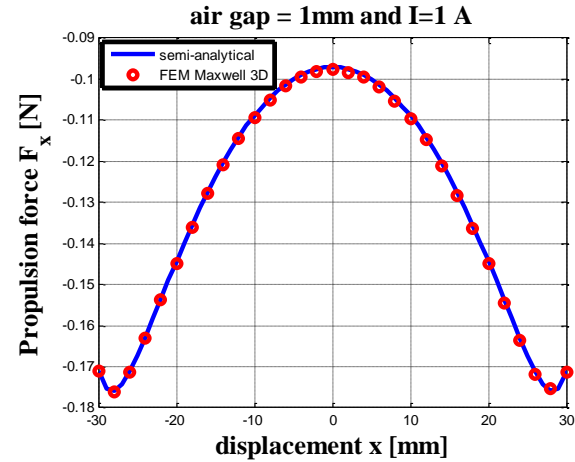


Fig. 9. Force-displacement curve of the propulsion coil.

IV. CONCLUSION

The new equation in this paper for determining the propulsion forces can help to evaluate the performance of our proposed 2-DoF actuator. It allows a very short calculation time compared to 3D-FEM and can be implemented very easy in MATLAB.

The results obtained by our new equation have been compared with 3D-FEM results. Both show a very good agreement with a maximum error of 1%.

The presented theory in this paper can also be used to derive similar semi-analytical equations for analysis, optimization and design issues of other ironless PM-actuators.

REFERENCES

- [1] H. Butler, "Position control in lithographic equipment," *IEEE Control System Magazine*, vol. 31, iss. 5, pp. 28-47, 2011.
- [2] L. Guang, Z. Yu, Z. Ming, D. Guanghong, and M. Tomizuka, "Six-DOF maglev nano precision microstage development," *IEEE International Conference on Mechanic Automation and Control Engineering (MACE)*, Wuhan, China, 2010.
- [3] M. Lahdo and S. Kovalev, "A novel high-precision magnetic levitation system," *Innovative Small Drives and Micro-Motor Systems*, Cologne, Germany, 2015.
- [4] H. Zhu, T. J. Teo, and C. K. Pang, "Conceptual design and modeling of a six degrees-of-freedom unlimited stroke magnetically levitated positioner," *IEEE/ASME International Conference on Advanced Intelligent Mechatronics (AIM)*, Besancon, France, pp. 1569-1574, 2014.
- [5] S. Verma, H. Shakir, and W.-J. Kim, "Novel electromagnetic actuation scheme for multi-axis nanopositioning," *IEEE Trans. on Magnetics*, vol. 42, no. 8, pp. 2052-2062, 2006.
- [6] A. V. Lebedev, E. A. Lomonova, P. G. Van Leuven, and J. Steinberg, "Analysis and initial synthesis of a novel linear actuator with active magnetic suspension," *Industry Applications Conference*, vol. 3, pp. 2111-2118, 2004.
- [7] Y. C. Lai, Y. L. Lee, and J. Y. Yen, "Design and servo control of a single-deck planar maglev stage," *IEEE Trans. on Magnetics*, vol. 43, iss. 6, pp. 2600-2602, 2007.
- [8] S. Mendaci, H. Allag, and M. R. Mekideche, "Multi-objective optimal design of surface-mounted permanent magnet motor using NSGA-II," *Applied Computational Electromagnets Society (ACES) Journal*, vol. 30, no. 5, May 2015.
- [9] J. W. Jansen, J. L. G. Janssen, J. M. M. Rovers, J. J. H. Paulides, and E. A. Lomonova, "(Semi-) analytical models for the design of high-precision permanent magnet actuators," *International Compu-mag Society Newsletter*, vol. 16, no. 2, pp. 4-17, 2009.
- [10] S. Wu, S. Zuo, X. Wu, F. Lin, and J. Shen, "Magnet modification to reduce pulsating torque for axial flux permanent magnet synchronous machines," *Applied Computational Electromagnets Society (ACES) Journal*, vol. 31, no. 3, Mar. 2016.
- [11] A. Shiri and A. Shoulaie, "Calculation of the magnetic forces between planar spiral coils using concentric rings," *Applied Computational Electromagnets Society (ACES) Journal*, vol. 25, no. 5, May 2010.
- [12] H. Jiang, X. Huang, G. Zhou, Y. Wang, and Z. Wang, "Analytical force calculation for high-precision planar actuator with Halbach magnet array," *IEEE Trans. on Magnetics*, vol. 45, no. 10, pp. 4543-4546, 2009.
- [13] J. W. Jansen, J. P. C. Smeets, T. T. Overboom, J. M. M. Rovers, and E. A. Lomonova, "Overview of analytical models for the design of linear and planar motors," *IEEE Trans. on Magnetics*, vol. 50, no. 11, 2014.
- [14] E. P. Furlani, "A formula for the levitation force between magnetic disks," *IEEE Trans. on Magnetics*, vol. 29, iss. 6, pp. 4165-4169, 1993.
- [15] S. Earnshaw, "On the nature of the molecular forces which regulate the constitution of the lumeniferous ether," *Trans. Cambridge Philos. Soc.*, vol. 7, pp. 97-112, Mar. 1839.



Mousa Lahdo received the diploma degree in Electrical Engineering from the University of Applied Sciences Mittelhessen in Friedberg, Germany, in 2012. Since then, he is a Research Associate and Ph.D. student at the Department of Mechatronics, Ilmenau University of Technology. His current research interests include magnetic bearings and magnetic levitation systems and novel integrated electro-mechanical actuators and motors for precision engineering systems.



Tom Ströhl researches at the Department of Mechatronics, Ilmenau University of Technology. He teaches Electrical Drive Systems as well as Mechanical and Fluid Actuators. He completed his Ph.D. on the subject of Model-Based Design of Electromagnets and he was involved in the development of the draft for the software SESAM. In numerous research and industrial projects, he gained experience in the design of electromagnetic drives and the magnetic measurement technology. He is co-author of several books on electromagnets and theoretical electrical engineering.



Sergej Kovalev is Professor for Electrical Drives, Electrical Engineering and Measurement Systems at the University of Applied Sciences in Friedberg, Germany, since 2012. He enrolled as a Ph.D. candidate in the Mechatronics Department at Technical University Ilmenau, Germany, in 1995 and received his Ph.D. degree in 2001. He has 14 years industrial experience in the R&D

departments at different firms in Germany. His research interest is the mechatronics of precision engineering, especially direct drives.